[논 문] 한국재료학회지
Kor. J. Mater. Res.
Vol. 22, No. 7 (2012)

http://dx.doi.org/10.3740/MRSK.2012.22.7.329

Effects of Cu and Ag Addition on Nanocluster Formation Behavior in Al-Mg-Si Alloys

JaeHwang Kim†, Hiroyasu Tezuka, Equo Kobayashi and Tatsuo Sato*

Department of Metallurgy and Ceramics Science, Tokyo Institute of Technology, 2-12-1, Ookayama, Meguro-ku, Tokyo, Japan
*Precision and Intelligence Laboratory, Tokyo Institute of Technology, 4259-R2-18, Nagatsuta, Midori-ku, Yokohama, Japan

(Received June 12, 2012 : Received in revised form June 18, 2012 : Accepted June 18, 2012)

Abstract Two types of nanoclusters, termed Cluster (1) and Cluster (2) here, both play an important role in the age-hardening behavior in Al-Mg-Si alloys. Small amounts of additions of Cu and Ag affect the formation of nanoclusters. Two exothermic peaks were clearly detected in differential scanning calorimetry(DSC) curves by means of peak separation by the Gaussian method in the base, Cu-added, Ag-added and Cu-Ag-added Al-Mg-Si alloys. The formation of nanoclusters in the initial stage of natural aging was suppressed in the Ag-added and Cu-Ag-added alloys, while the formation of nanoclusters was enhanced at an aging time longer than 259.2 ks(3 days) of natural aging with the addition Cu and Ag. The formation of nanoclusters while aging at 100°C was accelerated in the Cu-added, Ag-added and Cu-Ag-added alloys due to the attractive interaction between the Cu and Ag atoms and the Mg atoms. The influence of additions of Cu and Ag on the clustering behavior during low-temperature aging was well characterized based on the interaction energies among solute atoms and on vacancies derived from the first-principle calculation of the full-potential Korrinaga-Kohn-Rostoker(FPKKR)-Green function method. The effects of low Cu and Ag additions on the formation of nanoclusters were also discussed based on the age-hardening phenomena.

Key words Al-Mg-Si alloys, aging, nanoclusters, Cu addition, Ag addition.

1. Introduction

The age-hardenable Al-Mg-Si alloys have been widely used for body panels of automobiles due to their good formability, corrosion resistance and precipitation hardening response. With appearance of advanced equipments such as a three dimensional atom probe(3DAP), the study of nano-scale clusters in the initial stage of phase decomposition in the Al-Mg-Si alloys has become highly attractive. Yamada et al.[1] and Serizawa et al.[2] clearly revealed the existence of two types of nanoclusters, Cluster (1) and Cluster (2), in Al-Mg-Si alloys. The different characteristics of two types of nanoclusters such as the formation temperature,[2] growth behavior[2] and interaction with dislocations[3] affect the following aging behavior.[4] Yamada et al.[1] and Kim et al.[4] explained that the formation of Cluster (1) causes the negative effect of two-step aging while the formation of Cluster (2) prior to the formation of Cluster (1) suppresses the negative effect.

Addition of microalloying elements such as Cu[4,5] and Ag[6,7] strongly affects the formation of precipitates and mechanical properties. It is reported that the Cu-containing Al-Mg-Si alloys produce the QC,[8] QP,[8] Q',[9,10] L,[10,11] S[11] precipitates, while the Ag-containing Al-Mg-Si alloys produce the Ag-containing β'[12-14] phase. Sato et al.[15] emphasized the role of microalloying elements in the age-hardening behavior of the Al-based alloys with a proposal of "Nanocluster Assist Processing(NCAP)". However, the roles of Cu and Ag in the nanocluster formation behavior in Al-Mg-Si alloys are still poorly understood due to the very rapid formation of nanoclusters with extremely small size even though many researches[4-14] have been carried out on the age-hardening behavior by the Cu and Ag addition. The direct observation using an atom probe or 3DAP technique would be a powerful tool to understand the clustering behavior such as the chemical composition and size of nanoclusters, but the time required for the sample preparation make it difficult to observe the initial clustering behavior. In order to understand the clustering behavior, indirect observation such as the differential scanning calorimetry(DSC), positron annihilation lifetime spectroscopy(PALS), hardness and electrical resistivity measurements and computer simulation are quite useful methods to understand the early stage of the phase decomposition in Al-Mg-Si alloys. Furthermore, a first-principle calculation provides invaluable information to understand the atomic bonding behavior. With those requirements of the

†Corresponding author
E-Mail : kim.j.ai@m.titech.ac.jp (J. Kim)

systematic researches for understanding the early stage of the phase decomposition in Al-Mg-Si alloys, describing the initial clustering behavior through the indirect observation methods is still challenged. The present authors, therefore, aim to investigate the effects of the Cu and Ag addition on the nanocluster formation behavior in Al-Mg-Si alloys mainly through those indirect methods. The previously obtained results using 3DAP by Serizawa et al.[3] are basically utilized regarding the formation behavior of the two types of nanoclusters with the Cu and Ag addition. In order to elaborate the clustering behavior influenced by the Cu and Ag addition at the initial stage of phase decomposition, the obtained experimental results such as the hardness and electrical resistivity changes are discussed in terms of the interaction energies among solute atoms and vacancies.

2. Experimental Procedure

Four alloys named as Base, Cu-added, Ag-added and Cu-Ag-added are used in this study. Their chemical compositions are shown in Table 1. The solid solution heat treatment(ST) is performed at 560°C for 1.8 ks followed by quenching into the ice-water at 0°C for 60 s. Then, the single aging is performed at room temperature(natural aging, NA) or the isothermal aging at 100°C. DSC was operated using a Rigaku equipment of DSC823D/TAS-200 ranging from −50°C to 170°C with 30 mg Al (99.99%) as a reference under an argon atmosphere with a heating rate of 5°C/min. The DSC measurements just after ST are performed within 0.3 ks in order to minimize clustering during the sample preparation. Micro Vickers hardness measurements were employed using Mitsutoyo HM-102 within 0.3 ks after each heat treatment in order to minimize the NA effect. Seven hardness measurements for each data were acquired. The maximum and minimum values were ignored and the average of the remaining five was used. Meanwhile, other hardness measurements longer than 0.3 ks of NA are performed on time. The electrical resistivity measurements were performed at −196°C using liquid nitrogen by a four-probe method with 120 mA direct current. The specimen for the electrical resistivity measurement was put into liquid nitrogen within 1 or 2 s just after each heat treatment. Then, the electrical resistivity measurement is performed. The electrical resistivity results without time delay for the sample preparation may elaborate the initial clustering behavior.

Table 1. Chemical compositions of the alloys (at. %).

Alloy	Mg	Si	Cu	Ag	Fe	Al
Base	0.89	0.75	Tr.	Tr.	Tr.	Bal.
Cu-added	0.97	0.82	0.09	Tr.	Tr.	Bal.
Ag-added	0.98	0.81	Tr.	0.11	Tr.	Bal.
Cu-Ag-added	0.99	0.82	0.06	0.06	Tr.	Bal.

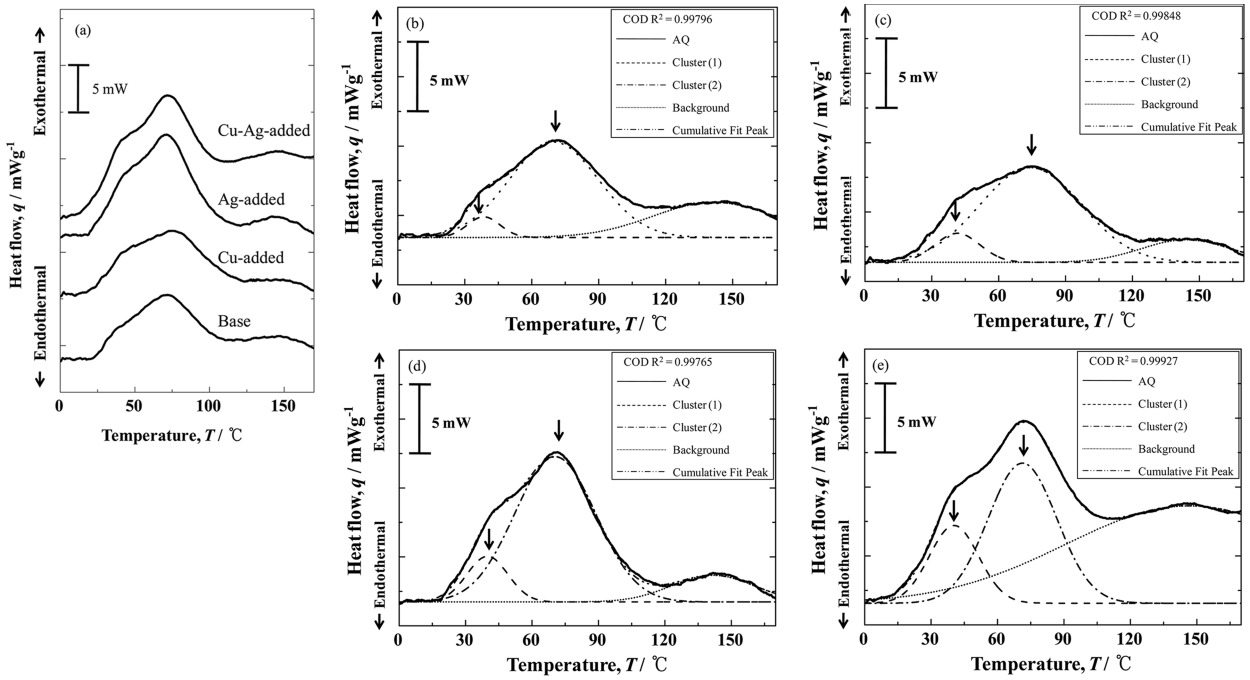

Fig. 1. DSC results of (a) the as-quenched specimens ranging from 0 to 170°C with heating rate of 5°C / min in the Base, Cu-added and Ag-added alloys. Peaks of nanoclusters are fitted by Gaussian function in the (b) Base, (c) Cu-added, (d) Ag-added and (e) Cu-Ag-added alloys.

3. Results

Fig. 1 shows the DSC results of the as-quenched specimens of the Base, Cu-added, Ag-added and Cu-Ag-added alloys ranging from 0 to 170°C with a heating rate of 5°C/min. The obtained DSC results are fitted by the Gaussian function in order to clearly understand the peak temperature of nanoclusters.[16] The peak point around 140°C in each curve in Fig. 1 is selected as a background of the DSC measurements in order to obtain the peak temperature by the Gaussian function. Two exothermic peaks indicated by arrows as shown in Figs. 1(b) to (e) appear at 38.4 and 69.9°C in the Base alloy, 41.4 and 74.3°C in the Cu-added alloy, 39.9 and 70.4°C in the Ag-added alloy, 40.4 and 71.3°C in the Cu-Ag-added alloy, respectively. Chang et al.[16] also obtained the peak temperature of nanoclusters using a similar method. Based on the previous 3DAP and DSC results[2] the lower temperature peak

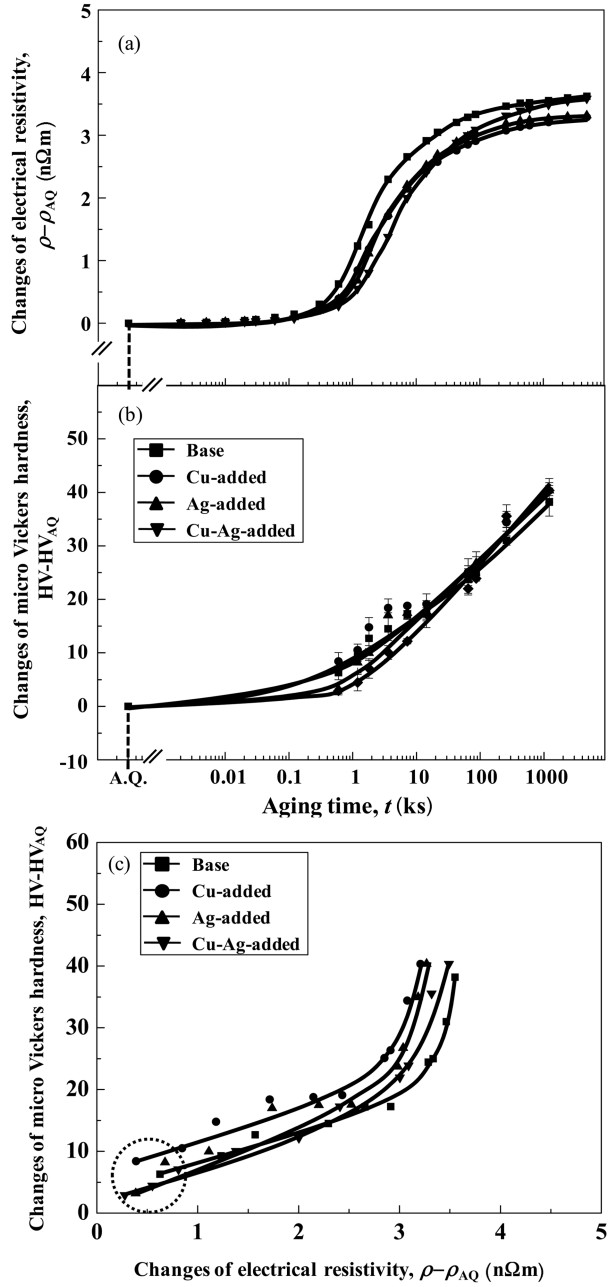

Fig. 2. Changes of the (a) electrical resistivity and (b) hardness during natural aging and (c) the changes of the hardness as a function of changes of electrical resistivity in the Base, Cu-added, Ag-added and Cu-Ag-added alloys.

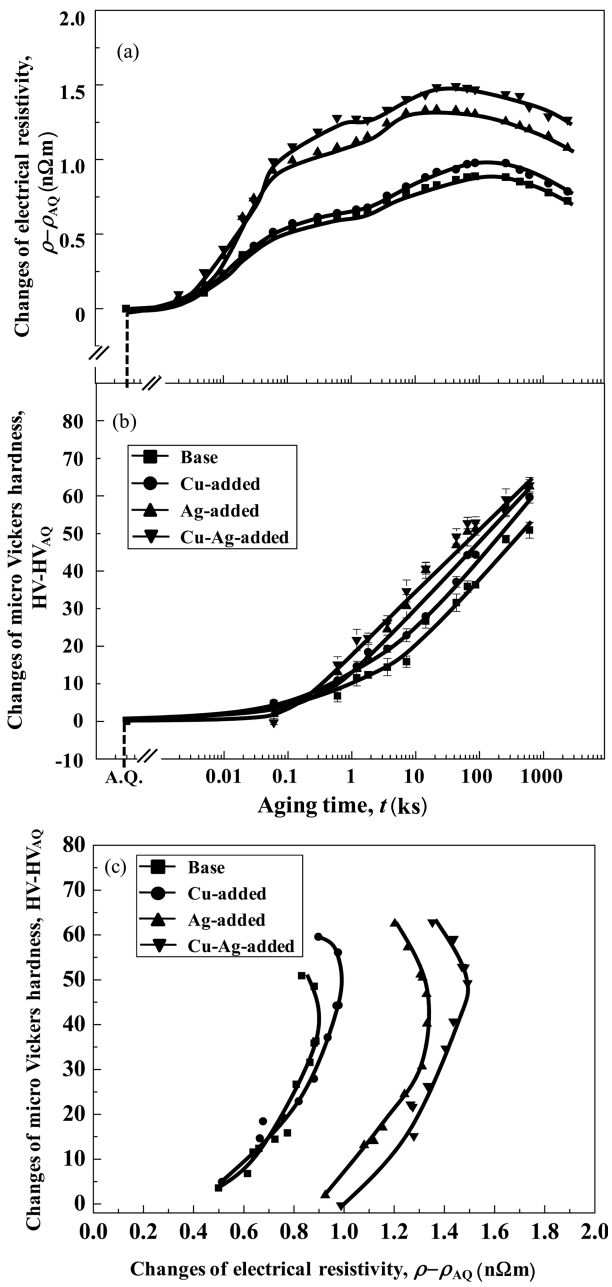

Fig. 3. Changes of the (a) electrical resistivity and (b) hardness during aging at 100°C and (c) the changes of the hardness as a function of changes of electrical resistivity in the Base, Cu-added, Ag-added and Cu-Ag-added alloys.

around 40°C can be assigned to Cluster (1) and the higher temperature peak around 70°C to Cluster (2).

Fig. 2 shows the changes of the electrical resistivity and hardness during NA in the Base, Cu-added, Ag-added and Cu-Ag-added alloys. The hardness and electrical resistivity changes are basically due to the formation of nanoclusters. As indicated by a circle in Fig. 2(c), the lower hardness and electrical resistivity changes at the initial NA are confirmed in the Ag-added and Cu-Ag-added alloys than the Base alloy. The slightly higher hardness obtained after NA for longer time than 259.2 ks (3 days) in the Cu-added, Ag-added and Cu-Ag-added alloys than the Base alloy as shown in Fig. 2(b).

Fig. 3 shows the changes of the electrical resistivity and hardness during aging at 100°C in the Base, Cu-added, Ag-added and Cu-Ag-added alloys. The Cu-added alloy shows a similar behavior to the Base alloy at the early stage of aging at 100°C in both the hardness and electrical resistivity changes. Electrical resistivity and hardness, however, increase more in the Cu-added alloy than in the Base alloy with increasing the aging time. On the other hand, the formation of Cluster (2) is greatly accelerated in the Ag-added and Cu-Ag-added alloys than the Base alloy from the initial aging at 100°C as shown in Fig. 2(c).

4. Discussions

Banhart et al.[17,18] divided the clustering behavior during NA into four stages based on the DSC and PALS analysis and assumed that the vacancy-solute complex is formed at the first stage of NA. Banhart et al.[17] also concluded that vacancies would be increasingly trapped and immobilized in the Si-rich clusters and then, the formation of the Mg-Si co-clusters is expected. Gupta et al.[19] and Chang et al.[16] explained that the Si-rich clusters are first formed and Mg atoms are incorporated into the Si-rich clusters during NA. Serizawa et al.[20] found experimentally using a 3DAP technique that the Si rich clusters bearing vacancies are formed at the initial stage of NA by the analysis of the inter-atomic distance between the solute atoms inside the nanoclusters. They also clarified that Mg atoms incorporate into the Si rich clusters with increasing the NA time. A similar clustering behavior to that already reported by Serizawa et al.[2,20] is considered to occur during NA in the Base alloy of the present study. The hardness increase is retarded up to 0.6 and 1.2 ks during NA in the Ag-added and Cu-Ag-added alloys as shown in Fig. 2(b). The formation of the Si rich clusters are suppressed by the Ag addition at the initial stage of NA since the hardness mainly increases due to the formation of nanoclusters. Maeguchi et al.[21] in our group also found that the electrical resistivity at the early stage of NA in the Ag-added alloy is lower than that in the Base alloy. In order to

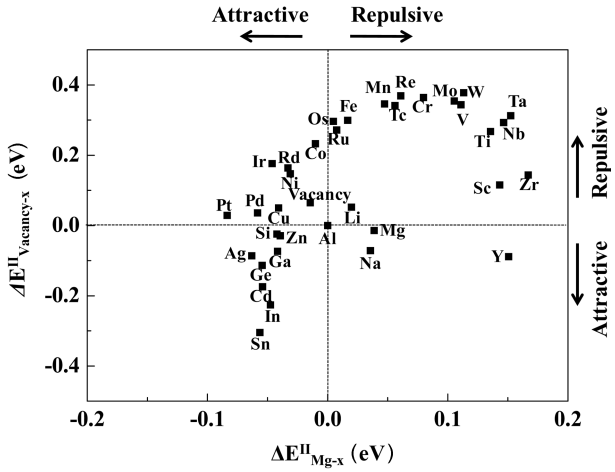

Fig. 4. Relationship between the nearest neighbor two-body interactions in Al derived from a first-principle calculation based on FPKKR-Green function method: ΔE^{II}_{Mgi-X} and $\Delta E^{II}_{Vacancy-X}$. See the text in detail.[22-27]

discuss reasonably the clustering behavior during NA, the interaction energies among solute atoms and vacancies are considered. The interaction energies are derived from the first-principle calculation based on the full-potential Korrinaga-Kohn-Rostoker(FPKKR)-Green function method. The energy difference of the nearest neighbor two-body interactions in Al between X and Y, ΔE^{II}_{X-Y}, is derived from the energy difference between the situations when the X and Y, i.e., microalloying elements or vacancies, are located in the nearest neighbor and infinitely far away on the aluminum lattice.[22-27] ΔE^{II}_{Mg-X} and $\Delta E^{II}_{Vacancy-X}$ in Fig. 4 represent the nearest neighbor two-body interactions in Al between Mg and X atoms and between vacancies and X atoms, respectively. X is labeled beside each plot, corresponding to a microalloying element or vacancy in Al-Mg-Si-X alloys.[22-27] Positive and negative values represent the repulsive and attractive interactions, respectively. Interaction energy maps provide valuable information to estimate the atomistic bonding at the initial stage of the phase decomposition in the age-hardenable Al-Mg-Si alloys. An expected clustering behavior in the age-hardenable Al alloys predicted by the interaction energies among solute atoms and vacancies is experimentally confirmed by the hardness, electrical resistivity measurements and 3DAP analysis in Al-Mg-Si,[28-30] Al-Cu,[30] Al-Cu-Mg,[28,29] Al-Zn,[31] Al-Zn-Ag[32] and Al-Zn-Mg[28,29] alloys in our group. Wolverton[33] also calculated the solute-vacancy bonding energies through the first-principle calculation based on the local density approximation and the generalized gradient approximation(GGA). It was found that Au, Si and Ag atoms, smaller than the Al atom, show strong binding energies with vacancies exceptionally since the lager solute atoms causing significant strain on the surrounding Al atoms would prefer to relax towards the vacancy to relieve

the strain.[33] Based on the first-principle calculation regarding the interactions among solute atoms and vacancies,[22-27,33] Sn, In Cd, Ge, Ag, Ga, Si and Zn show the attractive interactions with vacancies. Ag, Cd, In and Sn atoms strongly attract the vacancies based on the interaction energies[22-27,33] as shown in Fig. 4. Kimura et al.[34] proposed the vacancy trapping model, that is, Sn atoms trap vacancies resulting in retardation of the formation of GP zones in the Al-Cu alloys. It is worth noting that Ag atoms preferentially trap vacancies and retard the formation of Cluster (1). The low Cu addition would not strongly influence on the formation of Cluster (1) at the early stage of NA since Cu represents the repulsive interaction with vacancies. On the other hand, Cu and Ag atoms enhance the formation of nanoclusters at the aging time longer than 259.2 ks (3 days) of NA based on the hardness results as shown in Fig. 2. Torsæter[35] confirmed that Cu atoms are clearly incorporated into nanoclusters during NA for 7 days in the both Al-0.40% Mg-0.84% Si(Si-rich alloy) and Al-0.86% Mg-0.43% Si (Mg-rich alloy) alloys based on the 3DAP analysis. Furthermore, more pronounced Cu incorporation into the nanoclusters in the Mg rich alloy (NA for 7 days) than in the Si-rich alloys is confirmed.[35] Cu and Ag representing the strong attractive interactions with Mg can enhance the clustering behavior when Mg atoms are incorporated into the Si rich clusters during NA.

The formation of Cluster (2) at the early stage of aging at 100°C is enhanced in the Ag-added and Cu-Ag-added alloys than in the Base and Cu-added alloys as indicated in Fig. 3. Serizawa et al.[3] found that the average Cu and Ag concentration inside Cluster (2) is higher value than those of alloy compositions deducing that Cu and Ag atoms have strong interaction with solute atoms. It is noted that Cu and Ag having strong attractive interactions with Mg[22-27] accelerate the formation of Cluster (2) as shown in Fig. 3.

Osamura et al.[36] proposed the electrical resistivity change through the two-band model in an Al-Zn alloy. Based on their proposal, the electrical resistivity can be expressed as follows.

$$\rho = \rho_0 + \rho_M + \rho_P \quad (1)$$

where, ρ_0, ρ_M and ρ_P represent the electrical resistivity by the lattice vibration in the pure Al, solute atoms in the matrix and precipitates, respectively. ρ_0 does not change during isothermal aging. The term ρ_P highly contributes the total electrical resistivity changes compared with ρ_M during the low temperature aging. As a result, the electrical resistivity increases during the low temperature aging as shown in Figs. 2 and 3. The electrical resistivity by the solute atoms in the matrix can be described as follows.

$$\rho_M = \sum(\rho_s^0 \times C_s) \quad (2)$$

where, ρ_s^0 and C_S represent the average of the electrical resistivity per one weight percent of the remained solute atoms in the matrix and concentration of solute atoms, respectively. Yokota et al.[37] well summarized the effect of microalloying elements on the electrical resistivity and produced the average value of ρ_s^0 in Al alloys. The different values of ρ_s^0 for Cu and Ag also affects the electrical resistivity changes in Figs. 2 and 3. Further researches on the concentration chages of nanoclusters will elaborate the clustering behavior during the low temperature aging.

5. Conclusion

The effects of the Cu and Ag addition on the nanocluster formation behavior during the low temperature aging are investigated using DSC, electrical resistivity and hardness measurements in Al-Mg-Si alloys. The previously reported results are also discussed based on the Si rich clusters at the early stage of NA and Mg atoms incorporate into the nanoclusters as increasing the NA time.[2,17-20] The roles of Cu and Ag in the clustering behavior during natural aging(NA) and 100°C aging are discussed based on the interaction energies among solute atoms and vacancies derived from the first-principle calculation. The obtained results are summarized as follows.

1) The DSC curves of the as-quenched alloys are well fitted by the Gaussian function, indicating two peaks corresponding to Cluster (1) and Cluster (2). The formation behavior of nanoclusters are detected by the resistivity and hardness changes.

2) The formation of nanoclusters at the initial stage of NA is suppressed in the Ag-added and Cu-Ag-added alloys through the vacancy trapping since Ag represents the strong attractive interactions with vacancies. On the other hand, both the Cu and Ag enhance the formation of nanoclusters after NA for longer time than 259.2 ks (3 days).

3) The formation of nanoclusters from the initial stage of aging at 100°C is accelerated in the Ag-added and Cu-Ag-added alloys. Both the Cu and Ag accelerate the growth of nanoclusters with increasing the aging time.

Acknowledgements

Present authors are grateful to Furukawa-Sky Aluminum Corporation for the material supply and Tokyo Institute of Technology Global COE Program Education and Research Center for Material Innovation for the financial support.

References

1. K. Yamada, T. Sato and A. Kamio, J. Jpn. Inst. Light Met., **51**(4), 215 (2001) (in Japanese).
2. A. Serizawa, S. Hirosawa and T. Sato, Metall. Mater. Trans. A, **39**A, 243 (2008).
3. A. Serizawa, T. Sato and W. J. Poole, Phil. Mag. Lett., **90**, 279 (2010).
4. J. Kim, E. Kobayashi and T. Sato, Mater. Trans., **52**(5), 906 (2011).
5. S. Esmaeili, X. Wang, D. J. Lloyd and W. J. Poole, Metall. Mater. Trans. A, **34**A, 751 (2003).
6. K. Matsuda, K. Kido, T. Kawabata, Y. Uetani and S. Ikeno, J. Jpn. Inst. Light Met., **53**, 528 (2003) (in Japanese).
7. Y. Baba and A. Takashima, J. Jpn. Inst. Light Met., **19**(3), 90 (1969) (in Japanese).
8. C. Cayron, L. Sagalowicz, O. Beffort and P. A. Buffat, Phil. Mag. A, **79**(11), 2833 (1999).
9. K. Matsuda, S. Ikeno, Y. Uetani and T. Sato, Metall. Mater. Trans. A, **32**A, 1293 (2001).
10. D. J. Chakrabarti and D. E. Laughlin, Progr. Mater. Sci., **49**, 389 (2004).
11. C. D. Marioara, S. J. Andersen, T. N. Stene, H. Hasting, J. Walmsley, A. T. J. Van Helvoort and R. Holmestad, Phil. Mag., **87**(23), 3385 (2007).
12. K. Matsuda, , S. Ikeno, T. Sato and Y. Uetani, Scripta Mater., **55**, 127 (2006).
13. J. Nakamura, K. Matsuda, T. Kawabata, T. Sato, Y. Nakamura and S. Ikeno, Mater. Trans., **51**(2), 310 (2010).
14. C. D. Marioara, J. Nakamura, K. Matsuda, S. J. Andersen, R. Holmestad, T. Sato, T. Kawabata and S. Ikeno, Phil. Mag., **92**(9), 1149 (2012).
15. T. Sato, S. Hirosawa, K. Hirose and T. Maeguchi, Metall. Mater. Trans. A, **34**A, 2745 (2003).
16. C. S. T. Chang and J. Banhart, Metall. Mater. Trans. A, **42**A, 1960 (2011).
17. J. Banhart, C. S. T. Chang, Z. Liang, N. Wanderka, M. D. H. Lay and A. J. Hill, Adv. Eng. Mater., **12**, 559 (2010).
18. J. Banhart, M. D. H. Lay, C. S. T. Chang and A. J. Hill, Phys. Rev. B, **83**, 014101 (2011).
19. A. K. Gupta and D. J. Lloyd. Metall. Mater. Trans. A, **30**, 879 (1999).
20. A. Serizawa, W. J. Poole and T. Sato, Aluminium Alloys (ICAA-11) Vol. 1, p. 915, edited by J. Hirsch, B. Skrotzki, G. Gottstein, Wiley-VCH, USA (2008).
21. T. Maeguchi, K. Yamada and T. Sato, J. Jpn Inst. Metal., **66**(3), 127 (2002) (in Japanese).
22. T. Hoshino and F. Nakamura, J. Metastable Nanocrystalline Materials, **24-25**, 237 (2005).
23. S. Hirosawa, T. Omura, Y. Suzuki, T. Sato, Mater. Sci. Forum, 519-521, 215 (2006).
24. T. Hoshino, W. Schweika, R. Zeller and P. H. Dederichs, Phys. Rev. B, **47,** 5106 (1993).
25. M. Asato and T. Hoshino J. Jpn Inst. Metal., **63**(6), 676 (1999) (in Japanese).
26. T. Hoshino, T. Mizuno, M. Asato and H. Fukushima, Mater. Trans., **42**, 2206 (2001).
27. M. Asato, T. Mizuno, T. Hoshino and H. Sawada, Mater. Trans., **42**, 2216 (2001).
28. S. Hirosawa, F. Nakamura, T. Sato and T. Hoshino, J. Jpn. Inst. Light Met., **56**(11), 621 (2006) (in Japanese).
29. S. Hirosawa, F. Nakamura and T. Sato, Mater. Sci. Forum, **561-565**, 283 (2007).
30. T. Sato, K. Hirose and S. Hirosawa, in Proceedings of the 9th International Conference on Aluminum Alloys(Brisbane, Australia, August 2004), ed. J. F. Nie, A. J. Morton and B. C. Muddle(Institute of Materials Engineering Australasia), p. 956.
31. Y. Komiya, S. Hirosawa and T. Sato, Mater. Sci. Forum, **519-521**, 437 (2006).
32. T. Ogura, S. Hirosawa, A. Cerezo and T. Sato, Mater. Sci. Forum, **519-521**, 431 (2006).
33. C. Wolverton, Acta Mater., **55**, 5867 (2007).
34. H. Kimura and R. K. Hasiguti, Acta Metall., **9**, 1076 (1961).
35. M. Torsæter, Ph. D. Thesis, p. 101-105, Norwegian University of Science and Technology, Trondheim (2011).
36. K. Osamura, Y. Hiraoka and Y. Murakami, Phil. Mag., **28**(4), 809 (1973).
37. M. Yokota and K. Sato, J. Jpn. Inst. Light Met., **32**(8), 432 (1982) (in Japanese).